This article has been accepted for publication in a future issue of this journal, but has not been fully edited. Content may change prior to final publication. Citation information: DOI 10.1109/JRFID.2017.2739202, IEEE Journal of Radio Frequency Identification

Self-powered Multi-Port UHF RFID Tag-based-Sensor

Abdulhadi, *Member, IEEE,* and Tayeb A. Denidni , *Senier Member, IEEE,*

***Abstract*—In this paper, multi-port UHF RFID tag-based sensor for wireless identification and sensing applications is presented. Two RFID chips, one with attached sensor and the other without, are incorporated in a single tag antenna with two excitation ports. The chip with the integrated sensor (sensor port) transmits a signal impacted by the sensed temperature or humidity, while the other RFID chip serves as the reference signal (reference port) transmitter in the sensing process. The proposed tag-based sensor is fabricated and experimentally evaluated. The measured results demonstrate that the sensed data can be extracted using a commercial RFID reader by recording and comparing the difference in the reader output power required to power up the reference port and the power required to power the sensor ports. To improve the reading range of the proposed sensor, a dual-port solar powered RFID sensor is also presented. The reading range of the sensor is increased by two times compared to a similar prototype without solar energy harvesting. The experimental evaluation demonstrates that the proposed tag-based sensor can be easily integrated with a resistive humidity or temperature sensor for a low-cost solution to detect the heat or humidity exposure of sensitive items for several applications such as supply chains and construction structures.**

***Index Terms*—UHF RFID tag based-sensor, multi-port patch antenna for UHF RFID tag, RFID tag for wireless identification and sensing applications, Solar powered RFID tag-based sensor, RFID humidity and temperature sensors.**

I. Introduction

RFID technology has recently been employed in sensor applications that require low-cost low-power wireless nodes with radio identification and sensing capabilities [1]–[5]. Utilizing low-cost with long life time passive RFID tag-based sensor technology as an effective and reliable way for tracking and monitoring excess heat and humidity for several consumer items is gaining great interest in the scientific and industrial domains. Examples of low-cost RFID tag-based sensors that use off-the-shelf RFID chips and readers have been introduced in [2], [6]–[15]. The challenges in developing these types of sensors include designing suitable tag antennas and accurate determination of the sensed physical quantity (e.g. temperature, humidity, or permittivity) by using commercial RFID readers. In [2], [6]–[13], a pair of RFID tag antennas are employed for identification and sensing; one of the tags serves as a reference signal, while the other is used as a sensor node. The reference node has a common RFID tag configuration, while different approaches are adopted to implement the sensor node in [2], [5]–[14].

A. E. Abdulhadi is with the Department of Electrical and Computer Engineering, INRS, Montreal, Qc, H5A 1K6 Canada e-mail: (abdulhadi.abdulhadi@emt.inrs.ca).

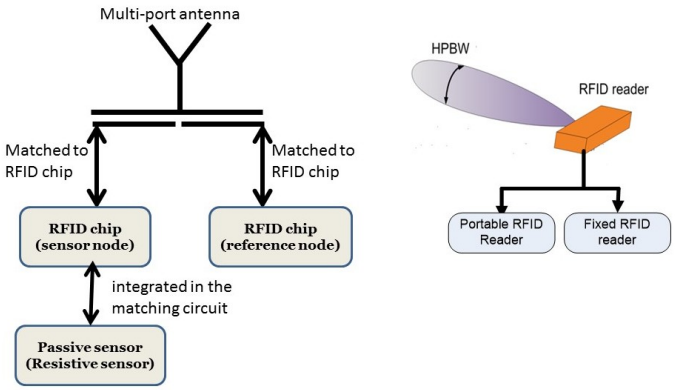

Fig. 1: Schematic diagram of the proposed RFID tag-based sensor.

The sensed physical quantity is determined from the ratio of the minimum power from the reader required to activate the reference and sensor nodes, or the power ratio of the signals received from reference and the sensor nodes. These values are then compared to benchmark laboratory experiments with the same tags, RFID chips and similar sensors [2], [5]–[14]. In [2], [6]–[12], the tag antennas are often dipole topology. Due to their omnidirectional radiation, these types of antennas are influenced by the characteristics of the identification object, and their resonance frequency, input impedance, radiation pattern and efficiency all degrade, especially when they are mounted on metallic surfaces or in close proximity to the human body [13]. These changes in the tag antenna characteristics affect the reference and the sensor nodes' signals, reducing the sensing accuracy, [13]. To overcome this problem, in [13], patch antennas have also been used for RFID sensors but still in a multiple tag arrangement [2], [5]–[13].

To reduce the cost, and the overall size of the developed sensor architecture, the sensor and reference ports must be integrated in one ordinary RFID tag. Including both reference and sensor nodes in the same antenna makes it possible to expose them to identical environmental conditions such as temperature. In addition, this ensures similar power levels for switches on the RFID chips, since a large separation between the sensor and reference nodes increases the risk of dissimilarity in the received powers due to propagation path variations. In this type of sensor architecture, the sensor nodes also limit the reading rang of the whole system, e.g., 1 m [6]. To increase the range, the sensor nodes' threshold power should be enhanced.

In this paper, a multi-port RFID tag-based sensor, operating at the 902-928 MHZ North American frequency band, is

This article has been accepted for publication in a future issue of this journal, but has not been fully edited. Content may change prior to final publication. Citation information: DOI 10.1109/JRFID.2017.2739202, IEEE Journal of Radio Frequency Identification

proposed. The proposed tag antennas are incorporated with multiple RFID chips (RI-UHF-IC116-00) provided by Texas Instruments, with power sensitivity of -13 dBm and input impedances of $8.2 - j61\Omega$ at the operation frequencies of 915 MHz, respectively. For a maximum power transfer between the RFID chips and the antennas, inductively-coupled loop and inset coupled feeds are integrated in each antenna layout. One port in each antenna is dedicated for attaching a resistive sensor as a load in parallel with the RFID chip. Few normal resistors are used as an alternate way to represent the resistive sensor in simulations and measurements. The proposed tag-based sensor is fabricated and experimentally evaluated using a commercial RFID test system. These tests show that the designed RFID tag sensor can read a resistance variation of between 20Ω to $2K\Omega$, which is equivalent to the resistance's variation of the humidity sensor (a write once read many WORM [6]) when there is a humidity change from 20% to 80%, or to the temperature sensors (NTC Thermistors [16]) whose resistances change from $1.9K\Omega$ (at 0^0C) up to 20.86Ω (at 145^0C). To improve the reading range of the sensor, a dual-port solar powered RFID-tag-enabled sensor is also fabricated and experimentally evaluated. The measured results demonstrate that the reading range of the dual-port solar powered RFID tag-enabled sensor is increased by two times compared to a similar prototype without solar energy harvesting. Compared to the author's earlier work on multi-port tag antenna [1], the proposed tag-based sensor is simpler, as it can be integrated with low-cost passive sensors without any additional discrete electronic components to measure different parameters (e.g. temperature or humidity).

This paper is organized as follows. The sensing principle of the proposed multi-port tag antenna is described in Section II. Next, the design and simulation results of the proposed tag antenna are presented in Section III. Experimental evaluations of the assembled tag-based sensor are provided in Section IV, followed by, a new multi-port solar powered RFID sensor that is described and experimentally evaluated in Section V. Finally, the conclusions are presented in Section VI.

II. Principle of the Multi port RFID tag based-sensor design

Passive RFID tags do not contain any power sources; Instead, they harvest the power required to operate the IC from the RF signal transmitted from the reader [17]. The amount of the power harvested by the tag strongly depends on the tag-antenna performance and the matching network between the chip and the tag antenna. The chip's impedance is highly capacitive ($Z_{in} = R_{Chip} - jX_{Chip}$); for the maximum power transfer conditions, the antenna input impedance must be conjugate matched to the microchip impedance ($Z_{Antenna} = Z^*_{Chip}$). The power transferred to the chip by the tag antenna can be represented as [11]:

$$P_{Tag} = \left(\frac{\lambda_0}{4\pi d}\right)^2 G_R(\theta,\varphi,\psi)\, G_T(\theta,\varphi,\psi)\, \tau P_t \eta_p \quad (1)$$

where λ_0 is the free space wavelength, d denotes the distance between the reader and the tag, G_T, and G_R represent the

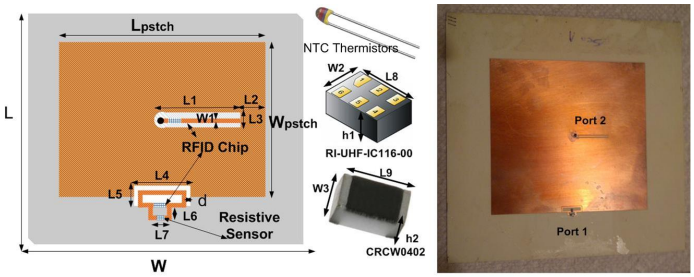

Fig. 2: Geometry of the proposed patch antenna-based sensor. All dimensions in millimeters (L_{Patch}= 83, W_{Patch}=79.6 , L=126 , W=126, L1=18.6 , L2=21, L3= 1.7, L4=11 , L5= 3.1, L6=1.5 , L7= 4.6, L8=1, L9=1 , W=79.6, W1=0.6, W2=0.5, W3=0.5, h1=0.55, h2=0.35, d=0.2.

tag and reader antenna gain, ψ is the environmental parameter that could affect the gain (i.e material [18], humidity [13] or [19], [20], temperature [21]), and τ is the power transmission coefficient of the tag, defined as:

$$\tau = \frac{4R_{Chip}R_{Antenna}(\psi)}{|Z_{Chip} + Z_{Antenna}(\psi)|^2} \quad (2)$$

The other parameters in Eq. 1 are P_t, the power transmitted from the RFID reader, and η_p , the polarization mismatch between the reader and the tag antenna.

The power received by the reader can be expressed by a radar equation [11]:

$$P_R = \left(\frac{\lambda_0}{4\pi d}\right)^4 G_R^2(\theta,\varphi,\psi)\, G_T^2(\theta,\varphi,\psi)\, \tau P_t \eta_p \rho(\psi) \quad (3)$$

where $\rho(\psi)$ is the modulation efficiency of the tag, which is a function of the antenna and chip impedances [22]. It is also related to the tag radar cross section as identified in [22]. The power received by the tag to activate the microchip or to be scattered by the tag is a function of the physical characteristics of the target where the tag is attached. Thus, any change in the target parameters causes a change in the power received by the tag as well as in the scattered power that is received by the reader. By detecting these changes, the target properties can be monitored in real time. However, preliminary laboratory experiments are needed to generate a calibrated reading of the backscattered signal from the sensor tag or the minimum power required from the reader to activate the tag.

The schematic diagram of the proposed multi-port RFID tag based sensor is shown in Fig. 1. The sensor port is integrated with a resistive moisture or resistive temperature sensor, [6] and [16], while the other port (the reference port) is perfectly matched to the tag antenna. Any change in the resistance of the sensor due to humidity or temperature variation introduces a mismatch between the antenna and the sensor port. The reader should then transmit a higher power level to activate the sensor port compared to that required for the reference port. Since the threshold power of the chips ($P_{C-threshold}$) is almost the same for the same types of chips and the reference and sensor ports are integrated in the same tag, the parameter of reader-to-tag distance can be dropped by calculating the ratio of the required minimum transmit power ($P_{t_{min}}$) to activate the two chips ($P_{Tag} \geq P_{C-threshold}$) (sensor and reference ports) using Eq.

This article has been accepted for publication in a future issue of this journal, but has not been fully edited. Content may change prior to final publication. Citation information: DOI 10.1109/JRFID.2017.2739202, IEEE Journal of Radio Frequency Identification

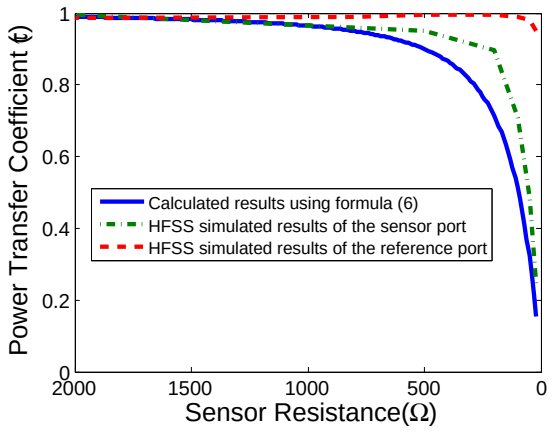

Fig. 3: Power transfer coefficient at the port of the proposed sensor with different resistors.

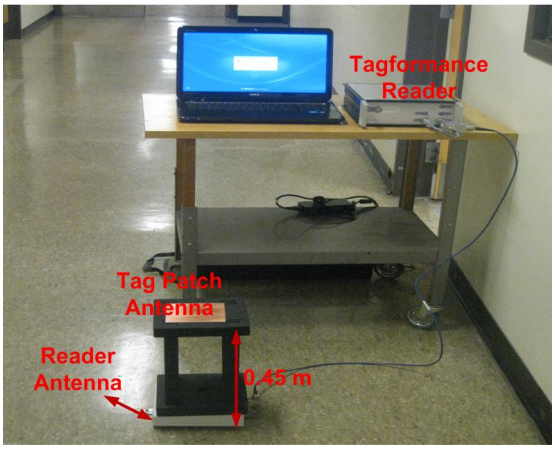

Fig. 4: Tagformance measurement setup

1. The calibration power up curve at any arbitrary distance from the reader can be obtained as follows:

$$P_{t_{min}}^{relative} = \frac{P_{t_{sensor}}}{P_{t_{reference}}} = \frac{\tau_{referencePort}}{\tau_{sensorPort}} \tag{4}$$

By measuring this power ratio, it is possible to map it to the sensor data and thereby the determine humidity or temperature at the tag location.

III. UHF RFID Sensor Tag Design

The tag antenna shown in Fig. 2 is designed and fabricated using a single layer substrate, Rogers RO4350B ($\varepsilon_r = 3.66$) with h= 1.524 mm to operate at the North American UHF RFID band (902-928 MHz). The length of the patch antenna is approximately one-half of a wavelength at the operating frequency of 915 MHz yielding L_{patch}=83mm and the width of W_{patch}=79.6mm. The overall dimensions of the tag including the ground plane are 126 mm x 126mm. To further reduce the footprint, the patch antenna is backed by an EBG structure as described by the authors in [23] and then redesigned with multiple feeds. In this manner, a size reduction of almost 70% (59mm x 79 mm) is obtained for the multi-port patch tag antenna. Multiple RFID chips (RI-UHF-IC116-00 [24]) provided by Texas Instruments are utilized. The power sensitivity of the chip is -13 dBm and the input impedance is $8.2 - j61\Omega$ at 915 MHz. The inductive loop and inset feed provide the conjugate match between the chips and the antenna ports. The port with an inset feed is chosen as the reference node. By changing the length of the inset feed (L1), the imaginary part of the input impedance is adjusted to yield a desired input impedance value. The real part is optimized by controlling the position of the via inside the patch antenna [23]. The second chip is connected to the antenna via an inductive loop. The size of the matching loop is adjusted to control the imaginary part, while the distance between the antenna and the loop affects the real part [25]. The final dimensions of the inset feed and the loop, as shown in Fig.1, are optimized using an HFSS simulator. The sensor can be directly connected to the tag antenna (in series or in parallel) [6] or it can be inductively coupled to the tag [7]. In this prototype, the sensor is directly connected to the matching loop in parallel with the RFID chip (See Fig. 2).

The reflection coefficient Γ of this port as seen by the RFID chip is [6]:

$$\Gamma = \frac{(Z_{Antenna} \parallel Z_{Sensor}) - Z_{Chip}^*}{(Z_{Antenna} \parallel Z_{Sensor}) + Z_{Chip}} \tag{5}$$

If the tag antenna is designed to be conjugate matched to the chip impedance ($Z_{Antenna} = Z_{Chip}^*$), the reflection coefficient (Γ) becomes:

$$\Gamma = \frac{-\left(Z_{Chip}^*\right)^2}{2Z_{Sensor}Re\left(Z_{Chip}\right) + \left|Z_{Chip}\right|^2} \tag{6}$$

Adding the resistive sensor in parallel with the sensor port introduces a mismatch ($|\Gamma|$ is larger than zero) between the antenna and the RFID chip. Thus, the power harvested from the RFID reader signals will not be completely transferred to the chip circuitry, as part of it will be reflected (the power transfer coefficient $\tau = 1 - |\Gamma|^2$). Compared to the reference port that is perfectly conjugate matched to the tag antenna, the reader requires to transmit higher power to activate the sensor port. According to Eq. 6 the reader will not be able to activate the sensor port when ($|\Gamma| = 1, Z_{Sensor} = 0$), while the best case to activate the sensor port (perfect conjugate matching) is when ($\Gamma = 0, Z_{Sensor} = \infty$). The proposed tag is simulated using an HFSS simulator where normal resistors (thick film chip resistors CRCW0402) with different resistance values ($2k\Omega$, $1k\Omega$, 500Ω, 200Ω, 100Ω, 50Ω, and 20Ω) are connected one at a time in the inductive loop as an alternative way to represent a resistive sensor (e.g. a Write Once Read Many WORM [6] or an NTCLE100E3681JB0 thermistor [16]). The calculated power transmission coefficient results using Eq. 6 and the simulated power transmission coefficient of the tag with these resistors are presented in Fig. 3. In both calculations using Eq.6 and an HFSS simulator, the chip impedance is set to be $8.2 - j61\Omega$ (provided in the component data sheet [24]), and the results are calculated at the center frequency of North American band (915 MHz). As expected, when the resistor values that are connected in parallel with the RFID chip, a mismatch between the chip and the antenna is introduced. The mismatch increases when the value of the resistor is decreased. There is a small variation in the power transmission coefficient

This article has been accepted for publication in a future issue of this journal, but has not been fully edited. Content may change prior to final publication. Citation information: DOI 10.1109/JRFID.2017.2739202, IEEE Journal of Radio Frequency Identification

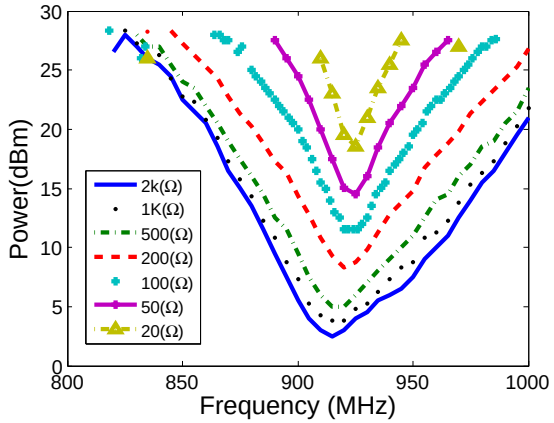

Fig. 5: Measured minimum transmit power required to activate RFID chip at the sensor port with different resistance values.

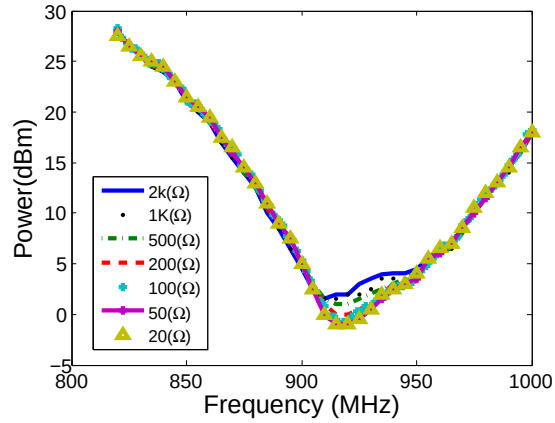

Fig. 6: Measured minimum transmit power required to activate RFID chip at the reference port with different resistance values.

at the reference port, but it is more than 94 % across the entire North American band. Thus, the reference port chip is expected to be activated with a minimum of power transmitted from the reader, and changing the resistance values at the sensor port does not have any impact as will be seen from the power sensitivity measurement in the next section.

IV. RFID TAG BASED-SENSOR EVALUATION

A. Power Sensitivity Measurements

Since sensor operation is based on measuring the relative activation power of the sensor and reference port chips, the power sensitivity measurement must be conducted in order to generate the calibration curve of the power-up levels. In addition, measuring the power sensitivity of the assembled tag provides information about the optimum operation frequency. Thus, any shifts in the resonance frequency because of antenna fabrication tolerances or RFID chip impedance tolerances due to parasitic effects, process variations or packaging can be observed. This test used a commercial RFID measurement system (Tagformance [26]). The measurement system is shown in Fig. 4, where the reader is connected to a computer to control the operation frequency band, the sweeping frequency step, and the maximum output power. The measurement system also includes a wide band circulator for monostatic

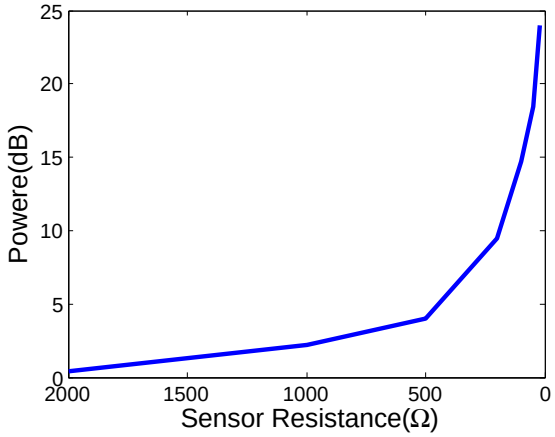

Fig. 7: Measured transmit power difference between sensor port and reference port at 915 MHz.

radar measurements with over 20 dB port isolation through a range of 800 to 1000 MHz. Tagformance was selected to perform the power sensitivity measurements because it covers broad operation frequency bands compared to a commercial RFID reader, e.g. GAO 216010 [27], which only operates in a narrow band from 865 to 868 MHz, European band, and 902 to 928 MHz, North America band. With this commercial reader (e.g. GAO 216010), the optimum operation frequency can not be predicted if it shifts out of the reader's operational bands. The tag is placed on the top of the foam holder at a 0.45 m distance from the reader, as shown in Fig. 4. The power sensitivity for the integrated RFID chips is then measured with different thick-film chip resistors (CRCW0402), i.e, $2k\Omega$, $1k\Omega$, 500Ω, 200Ω, 100Ω, 50Ω, and 20Ω, soldered one at a time for each port and each test to represent the resistive sensors. This process allows the power sensitivity of the sensor to be measured without the need for a climate room. The proposed sensor is measured across the 800-1000 MHz frequency band. The system starts by transmitting low power (-5 dBm) and then increases the output power by 0.1 dBm until the reader detects a tag response. The minimum transmit power needed to activate the sensor port was recorded for different resistance values and is plotted in Fig. 5.

It can be observed that the minimum power required from the reader (P_t) to activate the sensor port is inversely proportional to the sensor resistance. The sensor port is activated with a transmit minimum power of 2.5dBm when the sensor resistance is high ($2k\Omega$), while higher power (18.5 dBm) is needed when the sensor resistance is very low (20Ω). The required transmit power of the reference port is also measured for different resistance values connected at the sensor port. The measured results are presented in Fig. 6. The changes in the resistance values at the sensor port cause small changes in the transmit power required for activation (e.g., 1.5 dBm at 915 MHz when $R = 2k\Omega$, and -0.98dBm when $R = 20\Omega$) of the reference port due to the coupling effect between the two ports. These changes are already included in the calibration curve of the power-up levels and will not degrade the sensor accuracy. It can be seen that the optimum operation frequency of the proposed tag occurs at the center frequency

This article has been accepted for publication in a future issue of this journal, but has not been fully edited. Content may change prior to final publication. Citation information: DOI 10.1109/JRFID.2017.2739202, IEEE Journal of Radio Frequency Identification

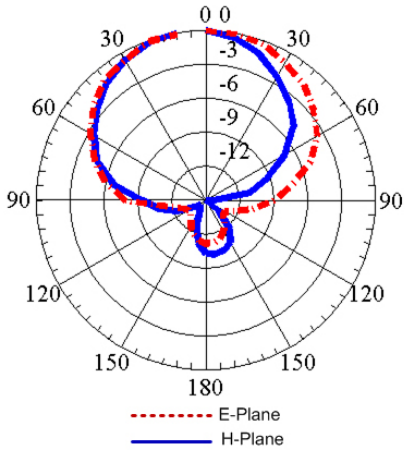

Fig. 8: Measured radiation pattern of the proposed sensor at 915 MHz.

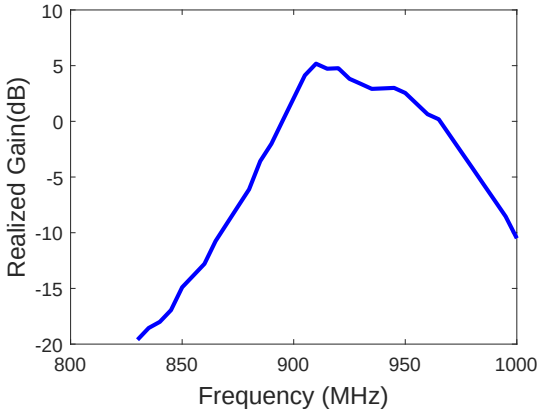

Fig. 9: Measured realized gain for the proposed tag-based sensor.

of the North American band, 915 MHz. At this operation frequency, a minimum transmitted power of -0.98 dBm is required to activate the RFID chip at the reference port. Thus, the differential power-up curve can be calculated using Eq. 4 at the operation frequency of (915 MHz), as presented in Fig. 7.

B. Reading range measurements

The other important parameter in evaluating an RFID tag is its maximum reading range. A tag's reading range can be easily measured using any commercial RFID reader. The same commercially-available measurement system (Tagformance) used above to measure the power consumption is used here for measuring the reading range. The maximum reading range (with an EIRP of 3.28 W at the reference port) using the proposed tags is 9 m. The calibrated curves of the differential power-up levels of the proposed sensor with a resistive sensor are measured at a distance of 0.45 m from the reader. A solar powered tag-based sensor was developed to enhance the reading range of the whole system, as explained in the next section.

C. Radiation pattern measurements

RFID tag antennas are loaded with the complex impedance of RFID chips, which is highly capacitive. This is not the standard setting (50Ω) in conventional pattern measurements, and therefore it is important to investigate the radiation pattern of the RFID tag antenna with an assembled and activated chip to observe any pattern deterioration. The Tagformance measurement system is used in an anechoic chamber to extract the radiation pattern from the power sensitivity measurements without any physical feed connection [26]. The radiation pattern of the proposed tag antenna at the operation frequency of 915 MHz is measured when both sensor and reference chips are connected. The measured results are presented in Fig. 8. The measured front-to-back ratio is 9.8 dB at 915 MHz. The realized antenna gain can be determined by using the power method presented in [28]. The realized gain of the proposed tag is presented in Fig. 9. The realized gain of the proposed tag antenna is 4.8 dB at 915 MHz.

TABLE I: Physical characteristics of Thermistors - NTCLE100E3681JB0

NTCLE100E3681JB0						
Temp.(^{0}C)	0	5	10	15	20	25
RT Ω	1941	1554	1253	1016	828.8	680.0
Temp.(^{0}C)	30	35	40	45	50	55
RT Ω	561.0	465.2	387.8	324.8	273.3	231.1
Temp.(^{0}C)	60	65	70	75	80	85
RT Ω	196.2	167.3	143.3	123.1	106.2	92.00
Temp.(^{0}C)	90	95	100	105	110	115
RT Ω	79.95	69.71	60.98	53.52	47.11	41.60

D. Sensor measurement results

In the first subsection of this tag-based sensor evaluation (Power Sensitivity Measurements), the proposed tags showed that they can successfully operate with a resistive sensor with a range of $2K\Omega$ to 20Ω. Currently, many different passive, compact and low-cost sensors that have similar resistance variations are available and suitable for direct integration with the proposed tag antennas. An example of a printed low-cost humidity or temperature sensor is a 1-bit write-once-read-many (WORM) presented in [5]–[7]. In our measurements, the proposed tag is integrated with another sensor available in our lab (Thermistors - NTC) [16] that has a similar resistance variation range to those described in [5]–[7], i.e., $1.9K\Omega$ at 0^0C to 196Ω at 60^0C. These types of sensors are not equipped with discrete electronic components that would increase the cost of the integrated sensor unit in the RFID tag; making them suitable for integration in a variety of consumer products in the proposed RFID tag sensor designs described earlier. Some of the physical characteristics of Thermistors - NTCLE100E3681JB0 are summarized in Table I. From Table I, it can be seen that at room temperature 25^0C, the available sensor has a resistor value of 680Ω. Since no climate room was available during the time of these measurements, the temperature sensor was only used to extract the power sensitivity of the proposed RFID sensor and to demonstrate the sensing principle of the RFID tag-based sensor operation, and not for the actual temperature measurements. The power sensitivities of the RFID chip at the sensor port and reference port are presented in Fig. 10. It can be seen that the sensor port requires higher power than the reference port, and that the ratio of the power transmitted to the sensor port to that

This article has been accepted for publication in a future issue of this journal, but has not been fully edited. Content may change prior to final publication. Citation information: DOI 10.1109/JRFID.2017.2739202, IEEE Journal of Radio Frequency Identification

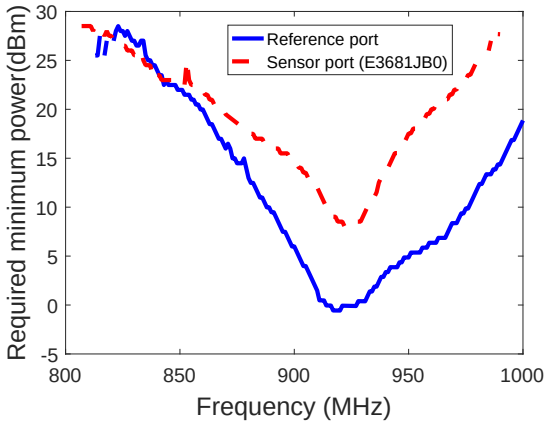

Fig. 10: Measured minimum transmit power required to activate RFID chip at the sensor port of the proposed RFID sensor with Thermistor - NTC NTC sensor.

transmitted to the reference port, can be extracted to determine the temperature if a calibration table or a climate room are available.

E. Power Sensitivity Measurements on Consumer Products

To demonstrate the use of the proposed tags-based sensor, measurements were conducted using two different types of packages. The measurement system (Tagformance) described in the earlier sections was also used to evaluate the performance of the proposed sensor with two different types of consumer products. As shown in Fig.11, the proposed sensor is attached to a box ($200 \times 200 \times 200mm$) containing plastic items, and then the RFID tag is attached to a box that filled with metallic cans. The tag is placed on top of the box at a distance of 0.45 m from the reader antenna of the measurement system. Since the principle method of sensing depends on the power sensitivity measurements, the tag is therefore first measured in free space and then attached to the two different packages. The measured results of the required minimum power for both ports in these two tests are presented in Figs.12 and 13. When the proposed sensor is attached to the top of a box containing plastic items, the minimum power needed to activate the RFID chips at the reference and sensor ports are very close to those of pertinent ports in free standing tag measurements. Thus, the loading effects of these types of items are negligible. However, when the proposed sensor is attached to the packages containing metallic objects, a small change in the minimum power for RFID chip activation is observed compared to the power required for free standing tags. For example, the required minimum power at 920 MHz for a sensor port is 8.4 dBm in a free standing tag, while it is 7 dBm when it is on the box containing metallic cans. The measured transmitted power difference between the sensor port and the reference port of free standing tags is 8.45 dB, while it is 8.05 dB when it is located on the box of metallic cans. Fig.14 presents the loading effect of the two different packages on a sample monopole RFID tag described in [29]. The loading effects of a box containing plastic items causes a large shift in the resonance frequency and increases the required minimum power compared to the proposed RFID tag-based sensor. The monopole antenna tag has a dramatically diminished performance when placed on the box containing metallic cans. Therefore, it can be observed that the proposed tag sensor is more immune to the loading effects of consumer products compared to RFID tags that use wire antennas for their sensor implementation [2], [5]–[14].

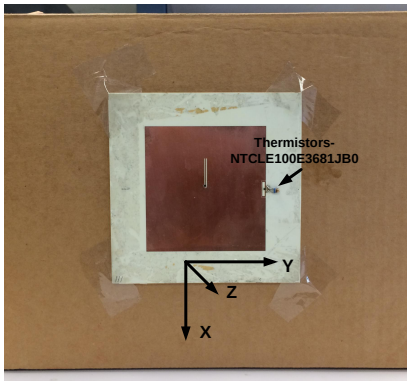

Fig. 11: Measured packages with Thermistors- NTCLE100E3681JB0.

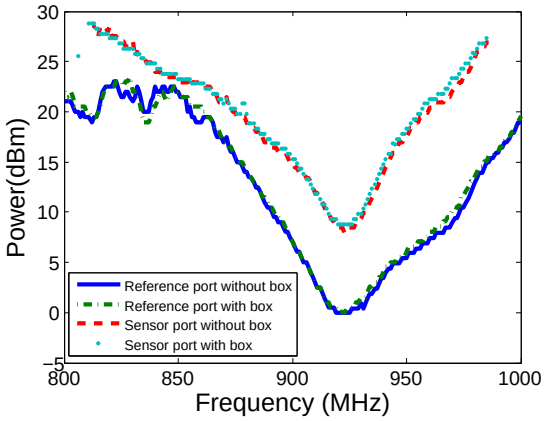

Fig. 12: Measured required minimum power for the reference and sensor ports of the tag in Fig. 11 attached to a box containing plastic items.

V. Solar Powered RFID Tag-Based Sensor

As mentioned in the previous section, sensor data is extracted from the power ratio described in Eq. 4. The power sensitivity measurements also confirm that the introduced mismatch due to the resistive sensor reduces the power sensitivity of the sensor port, with the reading range of the sensor port reduced accordingly. In fact, these types of sensors are general only suitable for use in short range applications, e.g., of 1 m [6]. Nonetheless, the reading range of the proposed sensors can be extended by improving the power sensitivity of both the reference and the sensor ports. Therefore, an improved design was developed herein. In this prototype, the power sensitivity of the IC is increased by including an additional energy source (solar cells [30]). A Monza X RFID chip with two pins for DC connection is used in the tag, which is designed to operate at the North American bandwidth (902 MHz to 928 MHz). A Rogers RO4350B substrate ($\varepsilon_r = 3.66$ and 1.524 thickness) is considered for implementing the tag antenna. At 915 MHz, the length and width of the radiating patch is optimized by

This article has been accepted for publication in a future issue of this journal, but has not been fully edited. Content may change prior to final publication. Citation information: DOI 10.1109/JRFID.2017.2739202, IEEE Journal of Radio Frequency Identification

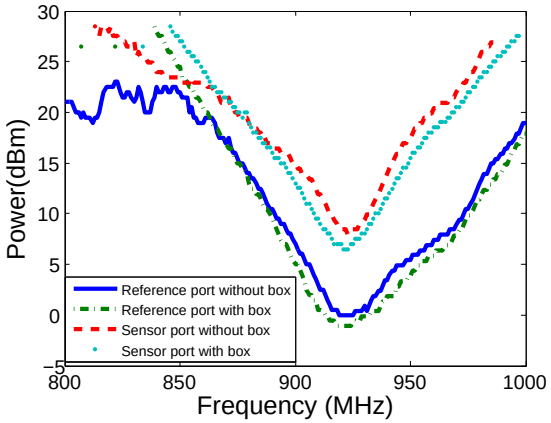

Fig. 13: Measured required minimum power for the reference and sensor ports of the tag in Fig. 11 attached to a box containing metallic items.

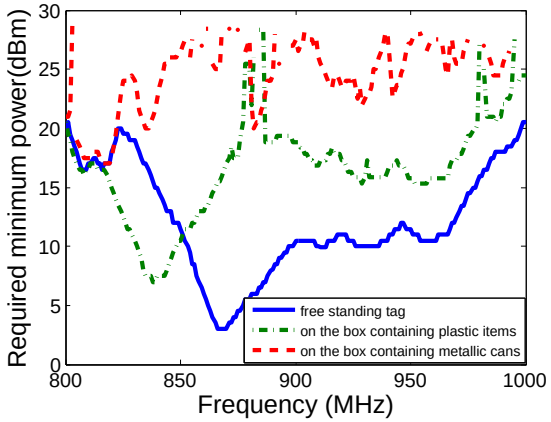

Fig. 14: Measured required minimum power for the monopole tag antenna described in [29] placed to the top of a box containing plastic and metallic items.

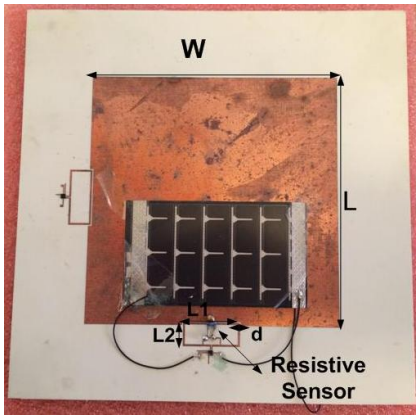

Fig. 15: Picture of the prototyped solar powered RFID tag-based sensor.

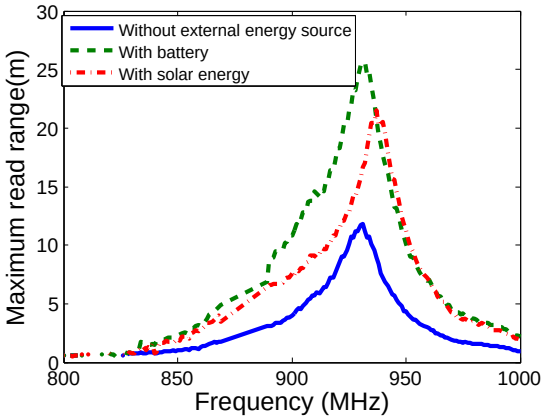

Fig. 16: Maximum reading range of the reference port with and without external energy sources.

using an HFSS simulator, yielding L=83 mm and W= 82.8 mm. The inductive loop matching technique is used to feed the RFID chip. The dimensions of the inductive loop are optimized for conjugate matching, resulting in L1=18.8 mm, L2=8.5mm, d=0.6 mm. A thin film of solar cells [31] are attached on the top of the patch antenna, as shown in Fig. 15. The dimensions of the solar panel are $64mm \times 37mm \times 0.2mm$, yielding an active area of $23cm^2$. As shown in Fig. 15, the DC+ and DC- of the solar panel are connected to the RFID using tiny wires.

The same system (TagFormance) that was used in the previous tag measurements is utilized here to evaluate the performance of the solar powered tag-based sensor. The reading ranges for the reference and sensor ports are measured with and without being connected to the solar energy source. First, the reading range of the RFID chip is measured without the external solar power source. Next, it is measured with two different external power sources connected, one at time: a small battery and the solar panel overlay. The measured reading range results for the reference port are presented in Fig.16. The maximum reading range without any additional energy source is obtained at 932 MHz (11.2 m), while with a small battery the maximum reading range is 25.6 m at 932 MHz (with an EIRP of 3.28 W). When the solar panel is used to power up the RFID chip under typical indoor office illumination conditions, a maximum reading range of 21.5 is achieved at 937 MHz (with an EIRP of 3.28 W). Due to the loading effect of the solar panel the maximum reading range is shifted from 932 MHz to 937 MHz. These measurements were repeated with a resistive thermal sensor, i.e., a Thermistor - NTCE100E3221JB0, connected in parallel with the RFID chip as shown in Fig. 15. The measured results of the maximum reading range are presented in Fig. 17. The reading range of the sensor port without an additional energy source is 2.4 m at 928 MHz. When the small battery and solar panel are used to power up the RFID chip, the reading ranges are 5.4 m at 928 MHz and 4.6 m at 934 MHz, respectively. It can be clearly observed that the effective reading range of the tag is almost doubled when an additional energy source is used to power up the RFID chip.

VI. Conclusion

The design and experimental evaluation of RFID tag-based sensors operating at UHF band were presented. The proposed sensor was designed to cover North America operation frequency band (902-928 MHz). Multiple RFID chips with operating frequencies from 840 MHz to 960 MHz and input impedances of $8.2 - j61\Omega$ at 915 MHz (North American band), were incorporated with the patch antenna. To achieve

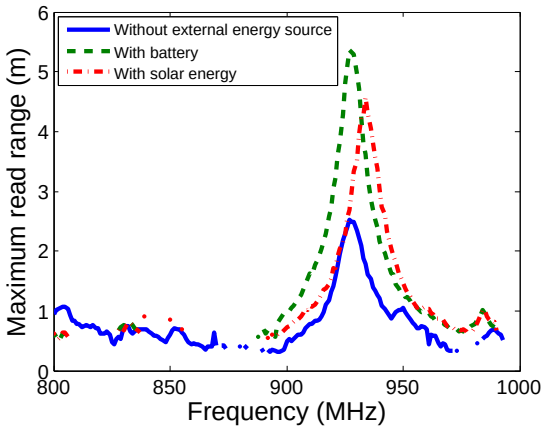

Fig. 17: Maximum reading range of the sensor port with and without external energy sources.

maximum power transfer between the chip and the antenna, unique matching mechanisms were implemented in the antenna layout. Utilizing these matching networks (inset feed and inductive loop), the patch antenna was conjugate matched to multiple RFID chips operating at an operation band of 902-928 MHz. To augment the sensing capability, resistive sensors were integrated in the same tags. The proposed tag-based sensor was fabricated and experimentally evaluated using a commercial measurement system. The measured front to back ratio is 9.8 dB at operation frequencies of 915 MHz, reducing the background tag materials' sensitivity. Thus, the proposed tag sensor is more immune to the loading effects of consumer products compared to RFID sensors based on wire antennas. The power sensitivity of the proposed sensor was also tested, and the preliminary calibrated curves of the differential power-up levels were obtained by measuring the differential power between the sensor and the reference ports. The maximum power ratio achieved by the proposed sensor is more than 23 dB at 0.45 m from the reader. To improve the reading range of the proposed sensor, a dual-port solar powered tag was fabricated and experimentally evaluated. The reading range was increased by two times compared to a similar prototype without solar energy harvesting. The measured results demonstrate that multi-port single tag antennas can reliably provide identification and sensing ability by monitoring the transmitted power of the reader. Thus, the proposed multi-port patch antennas equipped with resistive sensors are capable of serving as low-cost remote sensors for various applications including supply chain operations and the transportation of sensitive items.

REFERENCES

[1] A. E. Abdulhadi and R. Abhari, "Multiport UHF RFID-tag antenna for enhanced energy harvesting of self-powered wireless sensors," *IEEE Transactions on Industrial Informatics*, vol. 12, no. 2, pp. 801–808, 2016.

[2] S. Kim, Y. Kawahara, A. Georgiadis, A. Collado, and M. M. Tentzeris, "Low-cost inkjet-printed fully passive RFID tags for calibration-free capacitive/haptic sensor applications," *IEEE Sensors Journal*, vol. 15, no. 6, pp. 3135–3145, 2015.

[3] A. E. Abdulhadi, S. Mandev, and R. Abhari, "Signal integrity and EMI evaluations of an RFID-sensor tag for internet-of-things applications," in *2015 IEEE Symposium on Electromagnetic Compatibility and Signal Integrity*, 2015, pp. 128–132.

[4] L. Catarinucci, R. Colella, and L. Tarricone, "A cost-effective UHF RFID tag for transmission of generic sensor data in wireless sensor networks," *IEEE Transactions on Microwave Theory and Techniques*, vol. 57, no. 5, pp. 1291–1296, 2009.

[5] J. Gao, J. Sidn and H.-E. Nilsson, "Printed temperature sensors for passive RFID tags," *in Proc. 27th Conf. PIERS*, pp. 845–849, 2010.

[6] J. Gao, J. Siden, H. Nilsson, and M. Gulliksson, "Printed humidity sensor with memory functionality for passive RFID tags," *IEEE Sensors Journal*, vol. 13, no. 5, pp. 1824–1834, 2013.

[7] J. Gao, J. Siden, and H.-E. Nilsson, "Printed electromagnetic coupler with an embedded moisture sensor for ordinary passive RFID tags," *IEEE Electron Device Letters*, vol. 32, no. 12, pp. 1767–1769, 2011.

[8] J. Sidn, X. Zeng, T. Unander, A. Koptyug, and H.-E. Nilsson, "Remote moisture sensing utilizing ordinary RFID tags," in *IEEE Sensors*, 2007, pp. 308–311.

[9] Y. Jia, M. Hei, Q. Fu, and N. A. Gay, "A prototype RFID humidity sensor for built environment monitoring," in *2008 International Workshop on Education Technology and Training 2008 International Workshop on Geoscience and Remote Sensing*, vol. 2, 2008, pp. 496–499.

[10] A. Babar, S. Manzari, L. Sydanheimo, A. Elsherbeni, and L. Ukkonen, "Passive UHF RFID tag for heat sensing applications," *IEEE Transactions on Antennas and Propagation*, vol. 60, no. 9, pp. 4056–4064, 2012.

[11] G. Marrocco, L. Mattioni, and C. Calabrese, "Multiport sensor RFIDs for wireless passive sensing of objects-basic theory and early results," *IEEE Transactions on Antennas and Propagation*, vol. 56, no. 8, pp. 2691–2702, 2008.

[12] Z. Jiang and F. Yang, "Reconfigurable RFID tag antenna for wireless temperature monitoring," in *Proceedings of the 2012 IEEE International Symposium on Antennas and Propagation*, 2012, pp. 1–2.

[13] J. Sidn, J. Gao, and B. Neubauer, "Microstrip antennas for remote moisture sensing using passive RFID," in *2009 Asia Pacific Microwave Conference*, 2009, pp. 2375–2378.

[14] S. Caizzone, C. Occhiuzzi, and G. Marrocco, "Multi-chip RFID antenna integrating shape-memory alloys for detection of thermal thresholds," *IEEE Transactions on Antennas and Propagation*, vol. 59, no. 7, pp. 2488–2494, 2011.

[15] G. Marrocco and F. Amato, "Self-sensing passive RFID: From theory to tag design and experimentation," in *2009 European Microwave Conference (EuMC)*, 2009, pp. 001–004.

[16] Vishay BC Components. (2016, Nov. 15). Thermistors - NTC 680ohms. [Online]. Available: http://ca.mouser.com/ProductDetail/Vishay-BC-Components/NTCLE100E3681JB0/?qs=sGAEpiMZZMv9eKVyXEc252bhEBvG/NVPB3rFhL7a9yqMXY=

[17] G. Marrocco, "The art of UHF RFID antenna design: impedance-matching and size-reduction techniques," *IEEE Antennas and Propagation Magazine*, vol. 50, no. 1, pp. 66–79, 2008.

[18] G. Manzi and M. Feliziani, "Impact of UHF RFID IC impedance on the RFID system performances in presence of dielectric materials," in *2008 International Symposium on Electromagnetic Compatibility - EMC Europe*, 2008, pp. 1–6.

[19] A. Cataldo, G. Monti, E. De Benedetto, G. Cannazza, and L. Tarricone, "A noninvasive resonance-based method for moisture content evaluation through microstrip antennas," *IEEE Transactions on Instrumentation and Measurement*, vol. 58, no. 5, pp. 1420–1426, 2009.

[20] P. Soontornpipit, C. Furse, Y. C. Chung, and B. Lin, "Optimization of a buried microstrip antenna for simultaneous communication and sensing of soil moisture," *IEEE Transactions on Antennas and Propagation*, vol. 54, no. 3, pp. 797–800, 2006.

[21] R. Bhattacharyya, C. Floerkemeier, and S. Sarma, "RFID tag antenna based temperature sensing," in *IEEE International Conference on RFID*, 2010, pp. 8–15.

[22] P. Nikitin, K. V. S. Rao, and R. Martinez, "Differential rcs of RFID tag," *Electronics Letters*, vol. 43, no. 8, pp. 431–432, 2007.

[23] A. E. Abdulhadi, H. M. Tehran, and R. Abhari, "Design and characterization of a miniaturized patch antenna for passive UHF RFID applications," in *2012 IEEE/MTT-S International Microwave Symposium Digest*, 2012, pp. 1–3.

[24] Texas Instruments. (2016, Nov. 15). SMT EPC Gen2 IC RI-UHF-IC116-00,. [Online]. Available: http://media.digikey.com/pdf/Data/RI-UHG-IC116-00.pdf

[25] H. Choo and H. Ling, "Design of electrically small planar antennas using inductively coupled feed," *Electronics Letters*, vol. 39, no. 22, pp. 1563–1565, 2003.

[26] Voyantic Ltd. (2016, Nov. 15). Tagformance. [Online]. Available: http://www.voyantic.com/index.php?trg=home
[27] GAO RFID Inc. (2016, Nov. 15). RFID Reader, GAO216010. [Online]. Available: http://www.gaorfid.com/RFID-PDF/216010.pdf
[28] S. Caizzone and G. Marrocco, "RFID grids: Part II -experimentations," *IEEE Transactions on Antennas and Propagation*, vol. 59, no. 8, pp. 2896–2904, 2011.
[29] A. Abdulhadi and R. Abhari, "Design and experimental evaluation of miniaturized monopole UHF RFID tag antennas," *IEEE Antennas and Wireless Propagation Letters*, vol. 11, pp. 248–251, 2012.
[30] A. P. Sample, J. Braun, A. Parks, and J. R. Smith, "Photovoltaic enhanced UHF RFID tag antennas for dual purpose energy harvesting," *2011 IEEE International Conference on RFID*, pp. 146–153, 2011.
[31] Powerfilm INC. (2016, Nov. 15). Flexible thin-film. [Online]. Available: http://www.powerfilmsolar.com

Abdulhadi Ebrahim Abdulhadi was born in Bani Walid "Al Rusaifa", Libya. He received the B.Sc. degree in Microwave and Radar Engineering from the Faculty of Electronic Engineering, Bani Walid "Al Rusaifa", Libya, in 2007, he received his M.Sc. degree in Antennas and Electromagnetic Engineering from Concordia University, Montreal, Canada. He received his Ph.D. degree from McGill University, Montreal, QC, Canada. Currently, he is working as a postdoc at INRS, Montreal, Qc, Canada. His research activity has been mostly focused on the integration between sensors and RFID tags, the realization of compact UHF RFID tags, Electromagnetic Bandgap Structures (EBG), multi-feed tag antennas, integrated multi-antenna systems, solar-energy-assisted sensor-enhanced UHF RFID tags and new techniques for tag characterization, optimization, and design.

Tayeb A. Denidni received M. Sc. and Ph.D. degrees in electrical engineering from Laval University, Quebec City, QC, Canada, in 1990 and 1994, respectively. From 1994 to 2000, he was a Professor with the engineering department, Universit du Quebec in Rimouski (UQAR), Rimouski, QC, Canada, where he founded the Telecommunications laboratory. Since August 2000, he has been with the Institut National de la Recherche Scientifique (INRS), Universit du Quebec, Montreal, QC, Canada. He found RF laboratory at INRS-EM, Montreal. He has a great experience with antenna design and he is leading a large research group consisting of three research scientists, eight Ph. D students, and two M.Sc. students. He served as a principal investigator on many research project sponsored By NSERC, FCI and numerous industries. His current research areas of interest include reconfigurable antennas using EBG and FSS structures, dielectric resonator antennas, metamaterial antennas, adaptive arrays, switched multi-beam antenna arrays, ultra-wideband antennas, microwave and development for wireless communications systems. From 2008 to 2010, Dr. Denidni served as an Associate Editor for IEEE Transactions on Antennas Propagation. From 2005 to 2007, Dr. Denidni served as an Associate Editor for IEEE Antennas Wireless Propagation Letters. Since 2015, he has served as Associate Editor for IET Electronics Letters. Since 2004, he has been elevated to the grade of Senior Member of the IEEE.